Comment on "Laser ablation of Cu and plume expansion into 1 atm ambient gas" [J. Appl. Phys. 97, 063305 (2005)]

D. Autrique and V. Alexiades

Citation: Journal of Applied Physics **115**, 166101 (2014); doi: 10.1063/1.4872325
View online: http://dx.doi.org/10.1063/1.4872325
View Table of Contents: http://scitation.aip.org/content/aip/journal/jap/115/16?ver=pdfcov
Published by the AIP Publishing

Comment on "Laser ablation of Cu and plume expansion into 1 atm ambient gas" [J. Appl. Phys. 97, 063305 (2005)]

D. Autrique[1,a)] and V. Alexiades[2]
[1]*Department of Physics and Optimas Research Center, TU Kaiserslautern, 67653 Kaiserslautern, Germany*
[2]*Department of Mathematics, University of Tennessee, Knoxville, Tennessee 37996-1320, USA*

(Received 12 December 2013; accepted 4 March 2014; published online 30 April 2014)

A hydrodynamic model used for the study of ns-laser ablation in an ambient environment [Z. Chen and A. Bogaerts, J. Appl. Phys. **97**, 063305 (2005)] was investigated and compared with an in-house developed code. After a detailed analysis of the source code and the underlying theoretical framework, significant flaws were detected in the model. It was found that the respective model as well as the ones presented in some earlier and later manuscripts is not able to simulate the ablation process, i.e., target heating, material removal, breakdown, plasma formation, and plume expansion, self-consistently. The present findings indicate that their use should be discontinued when modeling the overall ablation process. Based on existing models in the literature, alternative theoretical pathways are proposed to facilitate future computational studies of ns-laser ablation. © *2014 AIP Publishing LLC*. [http://dx.doi.org/10.1063/1.4872325]

I. INTRODUCTION

In Ref. 1, the physical processes occurring during ns-laser ablation of a copper target immersed in an ambient environment consisting of helium were modelled. A hydrodynamic model was employed, assuming local thermodynamic equilibrium. The copper sample was irradiated by a 15 ns UV-laser pulse operating at 266 nm and a fluence of 7.5 J/cm^2.

Since the temporal and spatial distribution of the laser energy between the target and the ablated material determine both the qualitative and quantitative character of the ablation process at later times, it is clear that the theoretical description of plasma formation plays a crucial role in this model. The onset of plasma formation is governed by the interdependence of the ablation, the collisional and radiative processes, as well as the laser-induced absorption mechanisms.[2] This implies that the breakdown mechanism, the considered laser absorption coefficients, the energy balance, the employed thermodynamic relations as well as the boundary conditions are all important features in the modelling framework. Their respective implementations in the model will be discussed in Secs. II–VI.

II. LASER ABSORPTION MECHANISMS

In the respective,[1] preceding,[3,4] and subsequent[5,6] works, inverse Bremsstrahlung in the field of neutrals was identified as the dominant laser absorption mechanism. In Ref. 5, the authors attributed their findings to the high neutral species density near the target surface, encountered during the initial expansion stage as well as to uncertainties in the absorption cross section. These observations contradict collisional-radiative studies that underline the role of photo processes such as single-[7,8] and multi-photon ionization[9–12] as well as resonant and non-resonant photoexcitation[8] during UV-VIS laser-induced breakdown. The following absorption coefficient for electron-neutral inverse Bremsstrahlung, adopted from Ref. 13, was introduced:

$$\alpha_{\mathrm{IB}}^{\mathrm{e,n}} = \left(1 - e^{-\frac{h\nu_{\mathrm{las}}}{k_{\mathrm{b}}T}}\right) Q_{\mathrm{IB}}^{\mathrm{e,n}} n_{\mathrm{e}} n_{\mathrm{n}}, \quad Q_{\mathrm{IB}}^{\mathrm{e,n}} = 10^{-46}\mathrm{m}^5. \tag{1}$$

Here, T, n_{e}, and n_{n} denote the local equilibrium temperature and the number densities of the electrons and neutrals, respectively. The first term accounts for stimulated emission, whereas the second ($Q_{\mathrm{IB}}^{\mathrm{e,n}} = 10^{-46}\mathrm{m}^5$) should be interpreted as a rough, experimental estimate of the electron-neutral inverse Bremsstrahlung cross section. It was adopted from the work of Taylor and Caledonia,[14] who reported experimental cross sections for the constituents of air, at wavelengths taken in the far-infrared region. Hence, the related constant cannot be used when investigating a copper sample irradiated by UV-laser light.

In another chapter[15] of the same reference,[16] however, more elaborate theories for the calculation of the electron-neutral inverse Bremsstrahlung cross section were discussed.[17–21] If the electrons, characterized by temperature T_{e}, follow a Maxwell-Boltzmann distribution function f_{MB}, the net absorption cross section can be calculated as

$$Q_{\mathrm{IB}}^{\mathrm{e,n}}(T_{\mathrm{e}}, h\nu_{\mathrm{las}}) = \int_0^{\infty} K_{\mathrm{IB}}^{\mathrm{e,n}}(\epsilon, h\nu_{\mathrm{las}}) f_{\mathrm{MB}}(\epsilon, T_{\mathrm{e}}) d\epsilon. \tag{2}$$

$Q_{\mathrm{IB}}^{\mathrm{e,n}}$ can be obtained when the partial cross section $K_{\mathrm{IB}}^{\mathrm{e,n}}$ is known. Here, the work of Dalgarno and Lane[17] is of interest as it consists of an elegant quantum-mechanical derivation of $K_{\mathrm{IB}}^{\mathrm{e,n}}$ in which the zeroth-order elastic scattering cross section is approximated by the momentum transfer cross section. The final result is a variable cross section that depends on the electron energy ϵ and photon energy $h\nu_{\mathrm{las}}$:

a)Electronic mail: dautriqu@physik.uni-kl.de

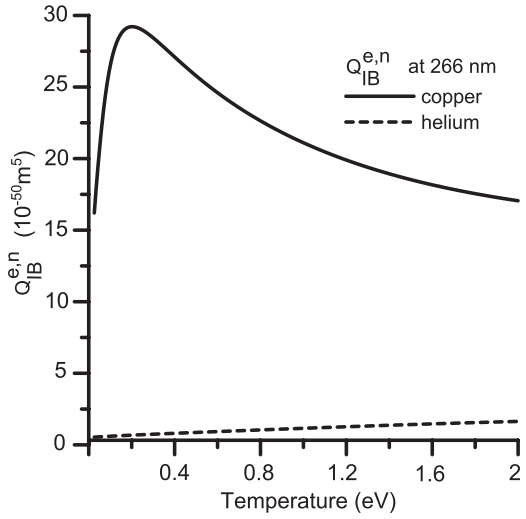

FIG. 1. Electron-neutral inverse Bremsstrahlung cross sections of copper and helium, taken at $\lambda_{las} = 266\,nm$, are shown.

$$K_{IB}^{e,n}(\epsilon, h\nu_{las}) = \frac{e^2}{12\pi^2 m_e c \nu_{las}^2 \epsilon_0}\sqrt{\frac{2(\epsilon + h\nu_{las})}{m_e}} \times \left[\frac{(\epsilon + h\nu_{las})}{h\nu_{las}}\sigma_m(\epsilon) + \frac{\epsilon}{h\nu_{las}}\sigma_m(\epsilon + h\nu_{las})\right], \tag{3}$$

where the elementary charge, the Planck constant, the electron mass, the vacuum permittivity, and the speed of light are represented by e, h, m_e, ϵ_0, and c, respectively. Fig. 1 depicts $Q_{IB}^{e,n}$ for copper and helium. The momentum transfer cross sections σ_m for both species in Eq. (3) were obtained from Refs. 22 and 23, respectively. The corresponding cross sections range as $\sigma_m = 10^{-14} - 10^{-15}\,cm^2$ in case of copper[22] and as $\sigma_m = 10^{-16} - 10^{-14}\,cm^2$ in case of helium.[23] The profiles of $Q_{IB}^{e,n}$, evaluated at $\lambda_{las} = 266\,nm$ and different electron temperatures, indicate that the respective cross sections are overestimated by up to four orders of magnitude.

Besides inverse Bremsstrahlung, photoionization was implemented in the model. The corresponding absorption coefficient was expressed as

$$\alpha_{PI} = \sigma_{PI} n_v, \quad \sigma_{PI} = 10^{-21} m^2. \tag{4}$$

Note that if Eq. (4) would hold, it would imply that single-photon ionization would take place, irrespective of the actual energy configuration of the vapor atoms. However, this can not be the case; as the first ionization potential of copper is 7.73 eV and a photon energy of 4.66 eV is considered, only neutral species that have electronic excitation energies above 3.13 eV would arrive in a higher charge state during single-photon ionization. It was found that Eq. (4) also appeared in Ref. 24. After having checked the corresponding source code of that work, it was noticed that single-photon ionization triggered breakdown artificially in the evaporated matter.[25] Hence, Eq. (4) needs substantial revision. If single-photon ionization is considered and if the photon energy exceeds the considered ionization energy, the following type of expression can be employed:[26]

$$\alpha_{PI} = \sum_{Z=0}^{Z_{max}-1}\sum_{i=N_*^Z}^{N_{max}^Z} n_i^Z \sigma_{PI,i}^Z. \tag{5}$$

Here, Z_{max} and N_{max}^Z denote the maximum charge and energy level numbers, respectively. The lower level limit, N_*^Z, indicates that the photon energy should at least exceed the binding energy of the respective atom in charge state Z. The photoionization cross section for a certain energy configuration, $\sigma_{PI,i}^Z$, can be calculated as[26,27]

$$\sigma_{PI,i}^Z = \frac{32\pi^2 Z^2}{3\sqrt{3}h^4 c \nu_{las}^3}\left(\frac{e^2}{4\pi\epsilon_0}\right)^3 \frac{u^{Z+1}(T_e)}{g_i^Z}\frac{dE_i^Z}{di}, \tag{6}$$

where u^{Z+1}, g_i^Z, and $\frac{dE_i^Z}{di}$, denote the partition function of the species in charge state $Z+1$, the statistical weight, and the spacing between the energy levels at the ith electronic level of the species in charge state Z, respectively. Finally, one can extend Eq. (5) and account for multi-photon ionization.[11,12] A total linear absorption coefficient, α_{MPI}, can then be found by deriving and linearizing the energy source term that corresponds to the multi-photon ionization rate.[28]

III. ENERGY BALANCE AND CLOSURE RELATIONS

Since the model should account for the different electronic energy configurations of the species, the energy balance and closure relations, specified in Ref. 1, should be modified accordingly. If local thermodynamic equilibrium (LTE) holds, the temperatures of the ions (T_{ion}), free (T_{el}), and bound (T_{exc}) electrons may be assumed equal; $T = T_{ion} = T_{el} = T_{exc}$. The number density of a certain species of charge Z residing in energy level i can now be obtained from the Boltzmann relation:

$$n_i^Z = n_0^Z \frac{g_i^Z}{g_0^Z} e^{-\frac{E_i^Z - E_0^Z}{k_b T}}. \tag{7}$$

Here, n_i^Z and n_0^Z denote the number densities of species of charge Z that reside in energy level i and ground state 0, respectively, whereas g_i^Z and g_0^Z are their corresponding statistical weights. Next, the ionization degree can be estimated from the Saha equation:[26]

$$\frac{n_e n^{Z+1}}{n^Z} = 2\left(\frac{2\pi m_e k_b T}{h^2}\right)^{\frac{3}{2}} \frac{u^{Z+1}(T)}{u^Z(T)} e^{-\frac{E_0^{Z+1} - E_0^Z}{k_b T}}, \tag{8}$$

where the total number densities of the electrons and species in charge states Z and $Z+1$ are given by n_e, n_Z, and n_{Z+1}, correspondingly. If the plasma mixture, consisting of copper (Cu) and helium (He), follows an ideal gas equation of state, the internal energy balance becomes

$$U = \frac{P}{\gamma - 1} + \sum_{l=Cu,He}\sum_{Z=0}^{Z_{max}^l}\sum_{i=0}^{N_{max}^{Z,l}} n_i^Z E_i^Z, \tag{9}$$

where the specific heat ratio, the internal energy density, and the total plasma pressure are represented by γ, U, and P, respectively.

```
F3(ix)=uB*(nVB*((1./gaM+xe(ix)*1.5)*kTB+xi1(ix)*Ip1+xi2(ix)*
(Ip1+Ip2))+nBB*((1./gaGM+x1(ix)*1.5)*KTB+x1(ix)*Ip1b)+
5)*(mV*nVB+mB*nBB)*uB**2+pB)
```

FIG. 2. Due to a mistyping in a continuation character of the employed Fortran 77 code at source line 655, the kinetic energy flux entering the plume domain at ix = 1 was overestimated tenfold (circle, red).

IV. BOUNDARY CONDITION

The target and the plasma in Ref. 1 were interconnected by a Knudsen layer.[29–31] Analytical relations for the temperature, density, and pressure ratios across the Knudsen layer were used to define the boundary conditions of the plume domain.[30] After a thorough investigation, it was found that the kinetic energy flux at the boundary was overestimated tenfold, see Fig. 2. As a result, a significant amount of energy entered the plume, inducing breakdown and plasma formation through Eqs. (8) and (9).

V. MODEL TESTS

In order to estimate the influence of the artifacts mentioned above, different test runs were carried out with the model of Ref. 1. Fig. 3 depicts temporal profiles of the surface temperature (solid) and near-surface plume temperature (dash) for different model settings.

In the original model (red, 1), the surface temperature of liquid copper stays well below its maximum (the critical temperature T_{crit}), whereas high plume temperatures are encountered. Here, a substantial amount of hot plasma is formed that tends to shield the sample surface from the incoming laser light. When the energy flux at the boundary (see Fig. 2) is corrected, both profiles (grey, 2) change drastically: the surface temperature rises and the plasma forms later.

When the laser absorption coefficients, $\alpha_{IB}^{e,n}$ and α_{PI}, are corrected and subsequently inserted (blue, 3), the profiles continue to change. Now, the surface temperature of liquid copper exceeds the critical temperature T_{crit} significantly. As a result, plasma formation is induced thermally by the overestimated surface temperature and surface pressure. Since the liquid-vapor line should end at the critical point, further revision is necessary. In a first approximation, one can assume that the hot liquid metal experiences a dielectric transition in the vicinity of the critical point and becomes transparent.[32] Provided that the equation of state of the near-surface target cells can be approximated by binodal relations, an evaporation front can at all times be attached to the target surface.[33] In this specific case (green, 4), the plume temperature (green, dash) above the sample surface does not exceed 0.5 eV, and neither breakdown nor plasma formation is encountered.

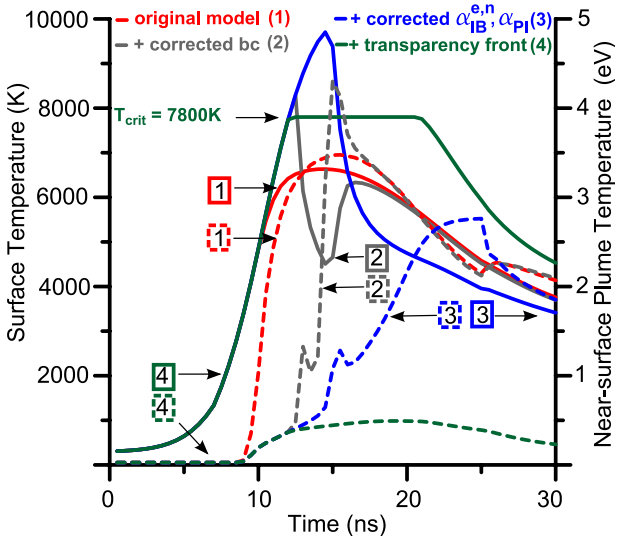

FIG. 3. Temporal profiles of surface (solid) and near-surface plume temperatures (dash) are shown for four model settings.

This demonstrates that the model under discussion cannot describe the ablation process self-consistently. Instead of assuming LTE *ad-hoc*, one needs to resolve the collisional and radiative mechanisms underlying laser-induced breakdown and plasma formation.[2,7,8,11,12] Assumptions with respect to eventual equilibria in the plasma can then be made *a posteriori*[34,35] and help to simplify the model.[8,12]

In a second step, the transparency assumption mentioned earlier should be omitted. As the target can arrive in near- or supercritical regions, a multiphase hydrodynamic approach should be employed.[36–38] Here, the insertion of a proper multiphase equation of state is an important step as it determines the actual response of the laser-irradiated material to the changing state variables.[39–42] Finally, a set of Euler equations can be solved throughout all material phases at once, i.e., solid, liquid, gas, and plasma.

VI. CONCLUSION

In summary, plasma formation and the subsequent expansion process are induced artificially in the model due to the superposition of three artifacts: an incorrect energy flux at the boundary (1), overestimated laser absorption coefficients (2), and an improper treatment of the liquid-vapor transition (3). If one attempts to study the whole ablation process, a collisional-radiative multiphase approach is indispensable.

Although the respective 1D LTE model cannot be employed for a self-consistent description of the overall ablation process, it can still be used to study the expansion process, *after* breakdown, *provided* that LTE holds. The latter Ansatz is approximately fulfilled during the early expansion stage following the end of the laser pulse.[12,43]

In that case, the model should be combined with a well-tailored experiment. By combining crater depth,[44,45] transmission,[44–47] and shadowgraphy[43–45,48] measurements, the initial mass, momentum, and energy densities of the plasma can be estimated and inserted in the model. The 1D spatial assumption can be fulfilled if a homogenized, flat-top laser profile is used. Since the spot size should at least exceed the plume length in this case, such model can only be applied for specific, early expansion stage studies.[49,50] For simulations encompassing longer expansion times, 2D axisymmetric[51–54] or even 3D model extensions[55] are necessary.

ACKNOWLEDGMENTS

David Autrique thanks Davide Bleiner for interesting discussions. Financial support from the Deutsche Forschungsgemeinschaft (Emmy Noether-Program, Grant RE 1141/11) is acknowledged.

[1]Z. Chen and A. Bogaerts, J. Appl. Phys. **97**, 063305 (2005).
[2]I. B. Gornushkin and U. Panne, Spectrochim. Acta, Part B **65**, 345 (2010).
[3]A. Bogaerts, Z. Chen, R. Gijbels, and A. Vertes, Spectrochim. Acta, Part B **58**, 1867 (2003).
[4]A. Bogaerts and Z. Chen, J. Anal. At. Spectrom. **19**, 1169 (2004).
[5]A. Bogaerts and Z. Chen, Spectrochim. Acta, Part B **60**, 1280 (2005).
[6]A. Bogaerts, Z. Chen, and D. Bleiner, J. Anal. At. Spectrom. **21**, 384 (2006).
[7]S. Amoruso, Appl. Phys. A: Mater. Sci. Process. **69**, 323 (1999).
[8]V. Mazhukin, V. Nossov, M. Nikiforov, and I. Smurov, J. Appl. Phys. **93**, 56 (2003).
[9]G. Weyl and D. Rosen, Phys. Rev. A **31**, 2300 (1985).
[10]D. Rosen and G. Weyl, J. Phys. D: Appl. Phys. **20**, 1264 (1987).
[11]V. Morel, A. Bultel, and B. Chéron, Spectrochim. Acta, Part B **65**, 830 (2010).
[12]D. Autrique, I. Gornushkin, V. Alexiades, Z. Chen, A. Bogaerts, and B. Rethfeld, Appl. Phys. Lett. **103**, 174102 (2013).
[13]R. G. Root, "Modelling of post-breakdown phenomena," in *Laser-Induced Plasmas and Applications* (Marcel Dekker, New York, 1989), pp. 69–103.
[14]R. L. Taylor and G. Caledonia, J. Quant. Spectrosc. Radiat. Transfer **9**, 657 (1969).
[15]G. M. Weyl, "Physics of laser-induced breakdown: An update," in *Laser-Induced Plasmas and Applications* (Marcel Dekker, New York, 1989), pp. 1–68.
[16]*Laser-Induced Plasmas and Applications*, edited by L. Radziemski and D. Cremers (Marcel Dekker, New York, 1989).
[17]A. Dalgarno and N. Lane, Astrophys. J. **145**, 623 (1966).
[18]Y. B. Zel'dovich and Y. P. Raizer, Sov. Phys. JETP **20**, 772 (1965).
[19]A. V. Phelps, "Theory of Growth of Ionization During Laser Breakdown," in *Physics of Quantum Electronics* (McGraw-Hill, New York, 1966), pp. 538–547.
[20]N. Kroll and K. M. Watson, Phys. Rev. A **5**, 1883 (1972).
[21]S. Geltman, J. Quant. Spectrosc. Radiat. Transfer **13**, 601 (1973).
[22]B. Chervy, O. Dupont, A. Gleizes, and P. Krenek, J. Phys. D: Appl. Phys. **28**, 2060 (1995).
[23]Y. Itikawa, At. Data Nucl. Data Tables **21**, 69 (1978).
[24]M. Aghaei, S. Mehrabian, and S. Tavassoli, J. Appl. Phys. **104**, 053303 (2008).
[25]M. Aghaei, private communication (2009).
[26]Y. B. Zel'dovich and Y. P. Raizer, *Physics of Shock Waves and High-Temperature Hydrodynamic Phenomena* (Dover, New York, 2002), Vols. 1 and 2.
[27]H. A. Kramers, Philos. Mag. **46**, 836 (1923).
[28]C. G. Morgan, Rep. Prog. Phys. **38**, 621 (1975).
[29]S. I. Anisimov, Sov. Phys. JETP **27**, 182 (1968).
[30]C. J. Knight, AIAA J. **17**, 519 (1979).
[31]A. V. Gusarov and I. Smurov, Phys. Fluids **14**, 4242 (2002).
[32]V. Batanov, F. Bunkin, A. Prokhorov, and V. Fedorov, Sov. Phys. JETP **36**, 311 (1973).
[33]J. H. Yoo, S. H. Jeong, R. Greif, and R. E. Russo, J. Appl. Phys. **88**, 1638 (2000).
[34]J. Van der Mullen, Phys. Rep. **191**, 109 (1990).
[35]G. Cristoforetti, A. De Giacomo, M. Dell'Aglio, S. Legnaioli, E. Tognoni, V. Palleschi, and N. Omenetto, Spectrochim. Acta, Part B **65**, 86 (2010).
[36]S. Anisimov and B. Luk'yanchuk, Phys. Usp. **45**, 293 (2002).
[37]D. Autrique, G. Clair, D. L'Hermite, V. Alexiades, A. Bogaerts, and B. Rethfeld, J. Appl. Phys. **114**, 023301 (2013).
[38]M. S. Qaisar and G. J. Pert, J. Appl. Phys. **94**, 1468 (2003).
[39]R. More, K. Warren, D. Young, and G. Zimmerman, Phys. Fluids **31**, 3059 (1988).
[40]A. V. Bushman, G. I. Kanel', L. A. Ni, and V. E. Fortov, *Intense Dynamic Loading of Condensed Matter* (Taylor & Francis, Washington, 1993).
[41]V. Fortov, K. Khishchenko, P. Levashov, and I. Lomonosov, Nucl. Instrum. Methods Phys. Res., Sect. A **415**, 604 (1998).
[42]P. R. Levashov and K. V. Khishchenko, Itteos 5.8 software for calculation of EOS for metals, 2007.
[43]M. Stapleton, A. McKiernan, and J.-P. Mosnier, J. Appl. Phys. **97**, 064904 (2005).
[44]G. Clair and D. L'Hermite, J. Appl. Phys. **110**, 083307 (2011).
[45]G. Clair, "Etudes théorique et expérimentale des plasmas produits par laser en vue de leur application à l'analyse chimique des matériaux en environment complexe," Ph.D. dissertation (Université d'Aix-Marseille II, 2011).
[46]A. Y. Vorob'ev, Sov. J. Quantum Electron. **15**, 490 (1985).
[47]N. M. Bulgakova and A. V. Bulgakov, Appl. Phys. A: Mater. Sci. Process. **73**, 199 (2001).
[48]A. V. Bulgakov and N. M. Bulgakova, J. Phys. D: Appl. Phys. **28**, 1710 (1995).
[49]A. Prokhorov, V. Konov, I. Ursu, and I. N. Mihailescu, *Laser Heating of Metals* (Adam Hilger, Bristol, 1990).
[50]D. Bäuerle, *Laser Processing and Chemistry* (Springer Verlag, Berlin, 2011).
[51]J. R. Ho, C. P. Grigoropoulos, and J. A. C. Humphrey, J. Appl. Phys. **78**, 4696 (1995).
[52]H. Le, D. Zeitoun, J. Parisse, M. Sentis, and W. Marine, Phys. Rev. E **62**, 4152 (2000).
[53]T. Itina, J. Hermann, P. Delaporte, and M. Sentis, Phys. Rev. E **66**, 066406 (2002).
[54]V. Mazhukin, V. Nossov, and I. Smurov, Thin Solid Films **453–454**, 353 (2004).
[55]S. I. Anisimov, *Instabilities in Laser-Matter Interaction* (CRC Press, Boca Raton, 1995).